6

TCO-Si Based Heterojunction Photovoltaic Devices

Z.Q. Ma[1] and B. He[2]
[1]*SHU-Solar E PV Laboratory, Department of Physics, Shanghai University, Shanghai*
[2]*Department of Applied Physics, Donghua University, Shanghai*
P. R. China

1. Introduction

It is a common viewpoint that the adscription of the PV research and industry in future has to be the lower cost and higher efficiency. However, those monocrystal as well as multi-crystalline silicon wafer require very expensive processing techniques to produce low defect concentrations, and they are made by complicated wet chemical treatment, high-temperature furnace steps, and time-cost metallization. Thus, a high PV module cost exists for the first-generation technology. Recently, a strong motivation in R&D roadmap of PV cells has been put forward in thin film materials and heterojunction device fields. A large variety of possible and viable methods to manufacture low-cost solar cells are being investigated. Among these strategies, transparent conductive oxides (TCOs) and polycrystalline silicon thin films are promising for application of PV and challenging to develop cheap TCOs and TCO/c-Si heterojunction cells.

Converting solar energy into electricity provides a much-needed solution to the energy crisis in the world is facing today. Solar cells (SC) fabricated on the basis of semiconductor–insulator– semiconductor (SIS) structures are very promising because it is not necessary to obtain a p–n junction and the separation of the charge carriers generated by the solar radiation is realized by the electrical field at the insulator–semiconductor interface. Such SIS structures are obtained by the deposition of thin films of TCO on the oxidized semiconductor surface. One of the main advantages of SIS based SC is the elimination of high temperature diffusion process from the technological chain, the maximum temperature at the SIS structure fabrication by PVD/CVD being not higher than 450 °C. Besides that, the superficial layer of silicon wafer, where the electrical field is localized, is not affected by the impurity diffusion. The TCO films with the band gap in the order of 2.5–4.5 eV are transparent in the whole region of solar spectrum, especially in the blue and ultraviolet regions, which increase the photo response in comparison with the traditional SC. The TCO layer assists the collection of charge carriers and at the same time is an antireflection coating. The most utilized TCO layers are SnO_2, In_2O_3 and their mixture ITO, as well as zinc oxide (ZnO). The efficiency of these kinds of devices can reach the value of more than 10% (Koida et al., 2009).

Transparent conducting oxides (TCOs), such as ZnO, Al-doped ZnO or ITO (SnO_2:In_2O_3), are an increasingly significant component in photovoltaic (PV) devices, where they act as electrodes, structural templates, and diffusion barriers, and their work function are

dominant to the open-circuit voltage. The desirable characteristics of TCO materials that are common to all PV technologies are similar to the requirements for TCOs for flat-panel display applications and include high optical transmission across a wide spectrum and low resistivity. Additionally, TCOs for terrestrial PV applications must be used as low-cost materials, and some may be required in the device-technology specific properties. The fundamentals of TCOs and the matrix of TCO properties and processing as they apply to current and future PV technologies were discussed.

As an example, the In_2O_3:SnO_2(ITO) transparent conducting oxides thin film was successfully used for the novel ultraviolet response enhanced PV cell with silicon-based SINP configuration. The realization of ultraviolet response enhancement in PV cells through the structure of ITO/SiO_2/np-Silicon frame (named as SINP), which was fabricated by the state of the art processing, have been elucidated in the chapter. The fabrication process consists of thermal diffusion of phosphorus element into p-type texturized crystal Si wafer, thermal deposition of an ultra-thin silicon dioxide layer (15-20Å) at low temperature, and subsequent deposition of thick In_2O_3:SnO_2 (ITO) layer by RF sputtering. The structure, morphology, optical and electric properties of the ITO film were characterized by XRD, SEM, UV-VIS spectrophotometer and Hall effects measurement, respectively.

The results showed that ITO film possesses high quality in terms of antireflection and electrode functions. The device parameters derived from current-voltage (I-V) relationship under different conditions, spectral response and responsivity of the ultraviolet photoelectric cell with SINP configuration were analyzed in detail. We found that the main feature of our PV cell is the enhanced ultraviolet response and optoelectronic conversion. The improved short-circuit current, open-circuit voltage, and filled factor indicate that the device is promising to be developed into an ultraviolet and blue enhanced photovoltaic device in the future.

On the other hand, the novel ITO/AZO/SiO_2/p-Si SIS heterojunction has been fabricated by low temperature thermally grown an ultrathin silicon dioxide and RF sputtering deposition ITO/AZO double films on p-Si texturized substrate. The crystalline structural, optical and electrical properties of the ITO/AZO antireflection films were characterized by XRD, UV-VIS spectrophotometer, four point probes, respectively. The results show that ITO/AZO films have good quality. The electrical junction properties were investigated by I-V measurement, which reveals that the heterojunction shows strong rectifying behavior under a dark condition. The ideality factor and the saturation current of this diode is 2.3 and 1.075×10^{-5}A, respectively. In addition, the values of I_F/I_R (I_F and I_R stand for forward and reverse current, respectively) at 2V is found to be as high as 16.55. It shows fairly good rectifying behavior indicating formation of a diode between AZO and p-Si. High photocurrent is obtained under a reverse bias when the crystalline quality of ITO/AZO double films is good enough to transmit the light into p-Si.

In device physics, the tunneling effect of SIS solar cell has been investigated in our current work, depending on the thickness of the ultra-thin insulator layer, which is potential for the understanding of quantum mechanics in the photovoltaic devices.

2. Review of TCO thin films

2.1 Development of TCOs

2.1.1 Feature of TCO

Most optically transparent and electrically conducting oxides (TCOs) are binary or ternary compounds, containing one or two metallic elements. Their resistivity could be as low as

10^{-5} Ω cm, and their extinction coefficient k in the visible range (VIS) could be lower than 0.0001, owing to their wide optical band gap (Eg) that could be greater than 3 eV. This remarkable combination of conductivity and transparency is usually impossible in intrinsic stoichiometric oxides; however, it is achieved by producing them with a non-stoichiometric composition or by introducing appropriate dopants. Badeker (1907) discovered that thin CdO films possess such characteristics. Later, it was recognized that thin films of ZnO, SnO_2, In_2O_3 and their alloys were also TCOs. Doping these oxides resulted in improved electrical conductivity without degrading their optical transmission. Al doped ZnO (AZO), tin doped In_2O_3, (ITO) and antimony or fluorine doped SnO_2 (ATO and FTO), are among the most utilized TCO thin films in modern technology. In particular, ITO is used extensively in acoustic wave device, electro-optic modulators, flat panel displays, organic light emitting diodes and photovoltaic devices.

The actual and potential applications of TCO thin films include: (1) transparent electrodes for flat panel displays (2) transparent electrodes for photovoltaic cells, (3) low emissivity windows, (4) window defrosters, (5) transparent thin films transistors, (6) light emitting diodes, and (7) semiconductor lasers. As the usefulness of TCO thin films depends on both their optical and electrical properties, both parameters should be considered together with environmental stability, abrasion resistance, electron work function, and compatibility with substrate and other components of a given device, as appropriate for the application. The availability of the raw materials and the economics of the deposition method are also significant factors in choosing the most appropriate TCO material. The selection decision is generally made by maximizing the functioning of the TCO thin film by considering all relevant parameters, and minimizing the expenses. TCO material selection only based on maximizing the conductivity and the transparency can be faulty.

Recently, the scarcity and high price of Indium needed for ITO materials, the most popular TCO, as spurred R&D aimed at finding a substitute. Its electrical resistivity (ρ) should be ~10^{-4} Ω cm or less, with an absorption coefficient (α) smaller than 10^4 cm^{-1} in the near-UV and VIS range, and with an optical band gap >3eV. A 100 nm thick film TCO film with these values for and will have optical transmission (T) 90% and a sheet resistance (R_S) of < 10 Ω/□.

At present, AZO and ZnO:Ga (GZO) semiconductors are promising alternatives to ITO for thin-film transparent electrode applications. The best candidates is AZO, which can have a low resistivity, e.g. on the order of 10^{-4} Ω cm, and its source materials are inexpensive and non-toxic. However, the development of large area, high rate deposition techniques is needed.

Another objective of the recent effort to develop novel TCO materials is to deposit p-type TCO films. Most of the TCO materials are n-type semiconductors, but p-type TCO materials are required for the development of solid lasers, as well as TFT or PV cells. Such p-type TCOs include: ZnO:Mg, ZnO:N, ZnO:In, NiO, NiO:Li, $CuAlO_2$, Cu_2SrO_2, and $CuGaO_2$ thin films. These materials have not yet found a place in actual applications owing to the stability.

Published reviews on TCOs reported exhaustively on the deposition and diagnostic techniques, on film characteristics, and expected applications. The present paper has three objectives: (1) to review the theoretical and experimental efforts to explore novel TCO materials intended to improve the TCO performance, (2) to explain the intrinsic physical limitations that affect the development of an alternative TCO with properties equivalent to those of ITO, and (3) to review the practical and industrial applications of existing TCO thin films.

2.1.2 Multiformity of TCOs

The first realization of a TCO material (CdO, Badeker 1907)) occurred slightly more than a century ago when a thin film of sputter deposited cadmium (Cd) metal underwent incomplete thermal oxidation upon postdeposition heating in air. Later, CdO thin films were achieved by a variety of deposition techniques such as reactive sputtering, spray pyrolysis, activated reactive evaporation, and metal organic vapor phase epitaxy (MOVPE). CdO has a face centered cubic (FCC) crystal structure with a relatively low intrinsic band gap of 2.28 eV. Note that without doping, CdO is an n-type semiconductor. The relatively narrow band gap of CdO and the toxicity of Cd make CdO less desirable and account for receiving somewhat dismal attention in its standard form. However, its low effective carrier mass allows efficiently increasing the band gap of heavily doped samples to as high as 3.35 eV (the high carrier concentration results in a partial filling of a conduction band and consequently, in a blue-shift of the UV absorption edge, known as the Burstein–Moss effect) and gives rise to mobility as high as 607 cm^2/V s in epitaxial CdO films doped with Sn. The high mobility exhibited by doped CdO films is a definite advantage in device applications. Cd-based TCOs such as CdO doped with either indium (In), tin (Sn), fluorine (F), or yttrium (Y), and its ternary compounds such as $CdSnO_3$, Cd_2SnO_4, $CdIn_2O_4$ as well as its other relevant compounds all have good electrical and optical properties. The lowest reported resistivity of Cd-based TCOs is 1.4×10^{-4} Ω cm, which is very good and competitive with other leading candidates. The typical transmittance of Cd-based TCOs in the visible range is 85%–90%. Although the Cd-based TCOs have the desired electrical and optical properties, in addition to low surface recombination velocity, which is very desirable, they face tremendous obstacles in penetrating the market except for some special applications such as CdTe/CdS thin film solar cells due to the high toxicity of Cd. It should be noted that the aforementioned solar cells are regulated and cannot be sold. To circumvent this barrier, the manufacturers lease them for solar power generation instead. Consequently, our attention in this chapter is turned away for discussing this otherwise desirable conducting oxide.

Revelations dating back to about 1960s that indium tin oxide (ITO), a compound of indium oxide (In_2O_3) and tin oxide (SnO_2), exhibits both excellent electrical and optical properties paved the way for extensive studies on this material family. In_2O_3 has a bixbyite-type cubic crystal structure, while SnO_2 has a rutile crystal structure. Both of them are weak n-type semiconductors. Their charge carrier concentration and thus, the electrical conductivity can be strongly increased by extrinsic dopants which is desirable. In_2O_3 is a semiconductor with a band gap of 2.9 eV, a figure which was originally thought to be 3.7 eV. The reported dopants for In_2O_3-based binary TCOs are Sn, Ge, Mo, Ti, Zr, Hf, Nb, Ta, W, Te, and F as well as Zn. The In_2O_3-based TCOs doped with the aforementioned impurities were found to possess very good electrical and optical properties. The smallest laboratory resistivities of Sn-doped In_2O_3 (ITO) are just below 10^{-4} Ω cm, with typical resistivities being about 1×10^{-4} Ω cm. As noted above, despite the nomenclature of Sn-doped In_2O_3 (ITO), this material is really an In_2O_3-rich compound of In_2O_3 and SnO_2. SnO_2 is a semiconductor with a band gap of 3.62 eV at 298 K and is particularly interesting because of its low electrical resistance coupled with its high transparency in the UV–visible region. SnO_2 grown by molecular beam epitaxy (MBE) was found to be unintentionally doped with an electron concentration for different samples in the range of $(0.3–3)\times10^{17}$ cm^{-3} and a corresponding electron mobility in the range of 20–100 cm^2/V s. Fluorine (F), antimony (Sb), niobium (Nb), and tantalum (Ta) are most commonly used to achieve high n-type conductivity while maintaining high optical transparency.

Much as ITO is the most widely used In_2O_3-based binary TCO, fluorine-doped tin oxide (FTO) is the dominant in SnO_2-based binary TCOs. In comparison to ITO, FTO is less expensive and shows better thermal stability of its electrical properties as well chemical stability in dye-sensitized solar cell (DSSC). FTO is the second widely used TCO material, mainly in solar cells due to its better stability in hydrogen-containing environment and at high temperatures required for device fabrication. The typical value of FTO's average transmittance is about 80%. However, electrical conductivity of FTO is relatively low and it is more difficult to pattern via wet etching as compared to ITO. In short, more efforts are beginning to be expended for TCOs by researchers owing to their above-mentioned uses spurred by their excellent electrical and optical properties in recently popularized devices. Germanium-doped indium oxide, IGO (In_2O_3:Ge), and fluorine-doped indium oxide, IFO (In_2O_3:F), reported by Romeo et al., for example, have resistivities of about 2×10^{-4} Ω cm and optical transmittance of ≥ 85% in the wavelength range of 400–800 nm, which are comparable to their benchmark ITO. Molybdenum-doped indium oxide, IMO (In_2O_3:Mo), was first reported by Meng et al.. Later on, Yamada et al. reported a low resistivity of 1.5×10^{-4} Ω cm and a mobility of 94 cm^2/V s, and Parthiban et al. reported a resistivity of 4×10^{-4} Ω cm, an average transmittance of >83% and a mobility of 149 cm^2/V s for IMO. Zn-doped indium oxide, IZO (In_2O_3:Zn), deposited on plastic substrates showed resistivity of 2.9×10^{-4} Ω cm and optical transmittance of ≥ 85%. Suffice it to say that In_2O_3 doped with other impurities have comparable electrical and optical properties to the above-mentioned data as enumerated in many articles.

The small variations existing among these reports could be attributed to the particulars of the deposition techniques and deposition conditions. To improve the electrical and optical properties of In_2O_3 and ITO, their doped varieties such as ITO:Ta and In_2O_3:Cd–Te have been explored as well. For example, compared with ITO, the films of ITO:Ta have improved the electrical and optical properties due to the improved crystallinity, larger grain size, and the lower surface roughness, as well as a larger band gap, which are more pronounced for ITO:Ta achieved at low substrate temperatures. The carrier concentration, mobility, and maximum optical transmittance for ITO:Ta achieved at substrate temperature 400°C are 9.16×10^{20} cm^{-3}, 28.07 cm^2/V s and 91.9% respectively, while the corresponding values for ITO are 9.12×10^{20} cm^{-3}, 26.46 cm^2/V s and 87.9%, respectively. Due to historical reasons, propelled by the above discussed attributes, ITO is the predominant TCO used in optoelectronic devices. Another reason why ITO enjoys such predominance is the ease of its processing. ITO-based transparent electrodes used in LCDs consume the largest amount of indium, about 80% of the total. As reported by Minami and Miyata (January, 2008), about 800 tons of indium was used in Japan in 2007. Because approximately 80%–90% of the indium can be recycled, the real consumption of indium in Japan in 2007 is in the range of 80–160 tons. The total amount of indium reserves in the world is estimated to be only approximately 6000 tons according to the 2007 United States Geological Survey. It is widely believed that indium shortage may occur in the very near future and indium will soon become a strategic resource in every country.

Consequently, search for alternative TCO films comparable to or better than ITO is underway. The report published by NanoMarkets in April 2009 (Indium Tin Oxide and Alternative Transparent Conductor Markets) pointed out that up until 2009 the ITO market was not challenged since the predicted boom in demand for ITO did not happen, partially due to the financial meltdown. The price of indium slightly varied from about US700$/kg in 2005 to US1000$/kg in 2007 and then to US700$/kg in 2009 which is still too expensive for

mass production. On the other hand, the market research firm iSupply forecasted in 2008 that the worldwide market for all touch screens employing ITO layers would nearly double, from $3.4 billion to $6.4 billion by 2013. Therefore, ITO as the industrial standard TCO is expected to lose its share of the applicable markets rather slowly even when alternatives become available. The report by NanoMarkets is a good guide for both users and manufacturers of TCOs.

In addition to ZnO-based TCOs, it also remarks on other possible solutions such as conductive polymers and/or the so-called and overused concept of nano-engineered materials such as poly (3, 4-ethylenedioxythiophene) well known as PEDOT by both H.C. Starck and Agfa, and carbon nanotube (CNT) coatings, which have the potentials to replace ITO at least in some applications since they can overcome the limitations of TCOs. Turning our attention now to the up and coming alternatives to ITO, ZnO with an electron affinity of 4.35 eV and a direct band gap energy of 3.30 eV is typically an n-type semiconductor material with the residual electron concentration of~10^{17} cm^{-3}. However, the doped ZnO films have been realized with very attractive electrical and optical properties for electrode applications. The dopants that have been used for the ZnO-based binary TCOs are Ga, Al, B, In, Y, Sc, V, Si, Ge, Ti, Zr, Hf, and F. Among the advantages of the ZnO-based TCOs are low cost, abundant material resources, and non-toxicity. At present, ZnO heavily doped with Ga and Al (dubbed GZO and AZO) has been demonstrated to have low resistivity and high transparency in the visible spectral range and, in some cases, even outperform ITO and FTO. The dopant concentration in GZO or AZO is more often in the range of 10^{20}–10^{21} cm^{-3} and although we obtained mobilities near 95 cm^2/V s in our laboratory in GZO typical reported mobility is near or slightly below 50 cm^2/V s. Ionization energies of Al and Ga donors (in the dilute limit which decreases with increased doping) are 53 and 55 meV, respectively, which are slightly lower than that of In (63 meV). Our report of a very low resistivity of~8.5×10^{-5} Ω cm for AZO, and Park et al. reported a resistivity of ~8.1×10^{-5} Ω cm for GZO, both of which are similar to the lowest reported resistivity of~7.7×10^{-5} Ω cm for ITO. The typical transmittance of AZO and GZO is easily 90% or higher, which is comparable to the best value reported for ITO when optimized for transparency alone and far exceeds that of the traditional semi-transparent and thin Ni/Au metal electrodes with transmittance below 70% in the visible range. The high transparency of AZO and GZO originates from the wide band gap nature of ZnO. Low growth temperature of AZO or GZO also intrigued researchers with respect to transparent electrode applications in solar cells. As compared to ITO, ZnO-based TCOs show better thermal stability of resistivity and better chemical stability at higher temperatures, both of which bode well for the optoelectronic devices in which this material would be used. In short, AZO and GZO are the TCOs attracting more attention, if not the most, for replacing ITO. From the cost and availability and environmental points of view, AZO appears to be the best candidate. This conclusion is also bolstered by batch process availability for large-area and large-scale production of AZO.

To a lesser extent, other ZnO-based binary TCOs have also been explored. For readers'convenience, some references are discussed at a glance below. B-doped ZnO has been reported to exhibit a lateral laser-induced photovoltage (LPV), which is expected to make it a candidate for position sensitive photo-detectors. In-doped ZnO prepared by pulsed laser deposition and spray pyrolysis is discussed, respectively. Y-doped ZnO deposited by sol–gel method on silica glass has been reported. The structural, optical and electrical properties of F-doped ZnO formed by the sol–gel process and also listed almost all the relevant activities in the field. For drawing the contrast, we should reiterate that among

all the dopants for ZnO-based binary TCOs, Ga and Al are thought to be the best candidates so far. It is also worth nothing that $Zn_{1-x}Mg_xO$ alloy films doped with a donor impurity can also serve as transparent conducting layers in optoelectronic devices. As well known the band gap of wurtzite phase of $Zn_{1-x}Mg_xO$ alloy films could be tuned from 3.37 to 4.05 eV, making conducting $Zn_{1-x}Mg_xO$ films more suitable for ultraviolet (UV) devices. The larger band gap of these conducting layers with high carrier concentration is also desired in the modulation-doped heterostructures designed to increase electron mobility. In this vein, $Zn_{1-x}Mg_xO$ doped with Al has been reported in Refs. The above-mentioned ZnO-based TCOs have relatively large refractive indices as well, in the range of 1.9–2.2, which are comparable to those of ITO and FTO. For comparison, the refractive indices of commercial ITO/glass decrease from 1.9 at wavelength of 400 nm to 1.5 at a wavelength of 800 nm, respectively. The high refractive indices reduce internal reflections and allow employment of textured structures in LEDs to enhance light extraction beyond that made feasible by enhanced transparency alone. The dispersion in published values of the refractive index is attributed to variations in properties of the films prepared by different deposition techniques. For example, amorphous ITO has lower refractive index than textured ITO. It is interesting to note that nanostructures such as nanorods and nanotips as well as controllable surface roughness could enhance light extraction/absorption in LEDs and solar cells, thus improving device performance. Fortunately, such nanostructures can be easily achieved in ZnO by choosing and controlling the growth conditions. One disadvantage of ZnO-based TCOs is that they degrade much faster than ITO and FTO when exposed to damp and hot (DH) environment. The stability of AZO used in thin film $CuInGaSe_2$ (CIGS) solar cells, along with Al-doped $Zn_{1-x}Mg_xO$ alloy, ITO and FTO, by direct exposure to damp heat (DH) at 85°C and 85% relative humidity. The results showed that the DH-induced degradation rates followed the order of AZO and $Zn_{1-x}Mg_xO \gg$ ITO > FTO. The degradation rates of AZO were slower for films of larger thickness which were deposited at higher substrate temperatures during sputter deposition, and underwent dry-out intervals. From the point of view of the initiation and propagation of degrading patterns and regions, the degradation behavior appears similar for all TCOs despite the obvious differences in the degradation rates. The degradation is explained by both hydrolysis of the oxides at some sporadic weak spots followed by swelling and popping of the hydrolyzed spots which are followed by segregation of hydrolyzed regions, and hydrolysis of the oxide–glass interfaces.

In addition to those above-mentioned binary TCOs based on In_2O_3, SnO_2 and ZnO, ternary compounds such as Zn_2SnO_4, $ZnSnO_3$, $Zn_2In_2O_5$, $Zn_3In_2O_6$, $In_4Sn_3O_{12}$, and multicomponent oxides including $(ZnO)_{1-x}(In_2O_3)x$, $(In_2O_3)_x(SnO_2)_{1-x}$, $(ZnO)_{1-x}(SnO_2)_x$ are also the subject of investigation. However, it is relatively difficult to deposit those TCOs with desirable optical and electrical properties due to the complexity of their compositions. Nowadays ITO, FTO and GZO/AZO described in more details above are preferred in practical applications due to the relative ease by which they can be formed. Although it is not within the scope of this article, it has to be pointed out for the sake of completeness that CdO along with In_2O_3 and SnO_2 forms an analogous In_2O_3–SnO_2–CdO alloy system. The averaged resistivity of ITO by different techniques is ~$1 \times 10^{-4}\Omega$•cm, which is much higher than that of FTO. For FTO, the typically employed technique is spray pyrolysis which can produce the lowest resistivity of ~3.8×10^{-4} Ω•cm. For AZO/GZO, the resistivities listed here are comparable to or slightly higher than ITO but their transmittance is slightly higher than that of ITO. Obviously, AZO and GZO as well as other ZnO-based TCOs are promising to replace ITO for transparent electrode applications in terms of their electrical and optical properties.There are also few

reports for some other promising n-type TCOs, which could find some practical applications in the future. They are titanium oxide doped with Ta or Nb, Ga_2O_3 doped with Sn and $12CaO \cdot 7Al_2O_3$ (often denoted $C_{12}A_7$). These new TCOs are currently not capable of competing with ITO/FTO/GZO/AZO in terms of electrical or optical properties. We should also point out that n-type transparent oxides under discussion are used on top of the p-type semiconductors and the vertical conduction between the two relies on tunneling and leakage. The ideal option would be to develop p-type TCOs which are indeed substantially difficult to attain.

3. Crystal chemistry of ITO

Crystalline indium oxide has the bixbyite structure consisting of an 80-atom unit cell with the Ia3 space group and a 1-nm lattice parameter in an arrangement that is based on the stacking of InO_6 coordination groups. The structure is closely related to fluorite, which is a face-centered cubic array of cations with all the tetrahedral interstitial positions occupied with anions. The bixbyite structure is similar to fluorite except that the MO_8 coordination units (oxygen position on the corners of a cube and M located near the center of the cube) of fluorite are replaced with units that have oxygen missing from either the body or the face diagonal. The removal of two oxygen ions from the metal-centered cube to form the InO_6 coordination units of bixbyite forces the displacement of the cation from the center of the cube. In this way, indium is distributed in two nonequivalent sites with one-fourth of the indium atoms positioned at the center of a trigonally distorted oxygen octahedron (diagonally missing O). The remaining three-fourths of the indium atoms are positioned at the center of a more distorted octahedron that forms with the removal of two oxygen atoms from the face of the octahedron. These MO_6 coordination units are stacked such that one-fourth of the oxygen ions are missing from each {100} plane to form the complete bixbyite structure. A minimum in the thin-film resistivity is found in the ITO system when the oxygen partial pressure during deposition is optimized. This is because doping arises from two sources, four-valent tin substituting for three-valent indium in the crystal and the creation of doubly charged oxygen vacancies. This is due to an oxygen-dependent competition between substitutional Sn and Sn in the form of neutral oxide complexes that do not contribute carriers. Amorphous ITO that has been optimized with respect to oxygen content during deposition has a characteristic carrier mobility (40 $cm^2/V\ s$) that is only slightly less than that of crystalline films of the same composition. This is in sharp contrast to amorphous covalent semiconductors such as Si, where carrier transport is severely limited by the disorder of the amorphous phase. In semiconducting oxides formed from heavy-metal cations with $(n-1)d^{10}ns^0$ ($n \leq 4$) electronic configurations, it appears that the degenerate band conduction is not band-tail limited.

4. ZnO thin films

Another important oxide used in PV window and display technology applications is doped ZnO, which has been learned to have a thin-film resistivity as low as $2.4 \times 10^{-4}\ \Omega \cdot cm$. Although the resistivity of ZnO thin films is not yet as small as the ITO standard, it does offer the significant benefits of low cost relative to In-based systems and high chemical and thermal stability. In the undoped state, zinc oxide is highly resistive because, unlike In-based systems, ZnO native point defects are not efficient donors. However, reasonable

impurity doping efficiencies can be achieved through substitutional doping with Al, In, or Ga. Most work to date has focused on Al - doped ZnO, but this dopant requires a high degree of control over the oxygen potential in the sputter gas because of the high reactivity of Al with oxygen. Gallium, however, is less reactive and has a higher equilibrium oxidation potential, which makes it a better choice for ZnO doping applications. Furthermore, the slightly smaller bond length of Ga–O (1.92Å) compared with Zn–O (1.97 Å) also offers the advantage of minimizing the deformation of the ZnO lattice at high substitutional gallium concentrations. The variety of ZnO thin films has been expatiated elsewhere.

5. Electrical conductivity of TCO

TCOs are wide band gap (Eg) semiconducting oxides, with conductivity in the range of 10^2 – 1.2×10^6 (S). The conductivity is due to doping either by oxygen vacancies or by extrinsic dopants. In the absence of doping, these oxides become very good insulators, with the resistivity of > 10^{10} Ω cm. Most of the TCOs are n-type semiconductors. The electrical conductivity of n-type TCO thin films depends on the electron density in the conduction band and on their mobility: $\sigma = \mu n e$, where μ is the electron mobility, n is its density, and e is the electron charge. The mobility is given by:

$$\mu = e \tau / m^* \quad (1)$$

where τ is the mean time between collisions, and m* is the effective electron mass. However, as n and τ are negatively correlated, the magnitude of μ is limited. Due to the large energy gap (Eg > 3 eV) separating the valence band from the conducting band, the conduction band can not be thermally populated at room temperature (kT~0.03 eV, where k is Boltzmann's constant), hence, stoichiometric crystalline TCOs are good insulators. To explain the TCO characteristics, the various popular mechanisms and several models describing the electron mobility were proposed.

In the case of intrinsic materials, the density of conducting electrons has often been attributed to the presence of unintentionally introduced donor centers, usually identified as metallic interstitials or oxygen vacancies that produced shallow donor or impurity states located close to the conduction band. The excess donor electrons are thermally ionized at room temperature, and move into the host conduction band. However, experiments have been inconclusive as to which of the possible dopants was the predominant donor. Extrinsic dopants have an important role in populating the conduction band, and some of them have been unintentionally introduce. Thus, it has been conjectured in the case of ZnO that interstitial hydrogen, in the H^+ donor state, could be responsible for the presence of carrier electrons. In the case of SnO_2, the important role of interstitial Sn in populating the conducting band, in addition to that of oxygen vacancies, was conclusively supported by first-principle calculations. They showed that Sn interstitials and O vacancies, which dominated the defect structure of SnO_2 due to the multivalence of Sn, explained the natural nonstoichiometry of this material and produced shallow donor levels, turning the material into an intrinsic n-type semiconductor. The electrons released by these defects were not compensated because acceptor-like intrinsic defects consisting of Sn voids and O interstitials did not form spontaneously. Furthermore, the released electrons did not make direct optical transitions in the visible range due to the large gap between the Fermi level and the energy level of the first unoccupied states. Thus, SnO_2 could have a carrier density with minor effects on its transparency.

The conductivity σ is intrinsically limited for two reasons. First, n and τ cannot be independently increased for practical TCOs with relatively high carrier concentrations. At high conducting electron density, carrier transport is limited primarily by ionized impurity scattering, i.e., the Coulomb interactions between electrons and the dopants. Higher doping concentration reduces carrier mobility to a degree that the conductivity is not increased, and it decreases the optical transmission at the near-infrared edge. With increasing dopant concentration, the resistivity reaches a lower limit, and does not decrease beyond it, whereas the optical window becomes narrower. Bellingham were the first to report that the mobility and hence the resistivity of transparent conductive oxides (ITO, SnO_2, ZnO) are limited by ionized impurity scattering for carrier concentrations above 10^{20} cm^{-3}. Ellmer also showed that in ZnO films deposited by various methods, the resistivity and mobility were nearly independent of the deposition method and limited to about 2×10^{-4} Ω cm and 50 cm^2/Vs, respectively. In ITO films, the maximum carrier concentration was about 1.5×10^{21} cm^{-3}, and the same conductivity and mobility limits also held. This phenomenon is a universal property of other semiconductors. Scattering by the ionized dopant atoms that are homogeneously distributed in the semiconductor is only one of the possible effects that reduce the mobility. The all recently developed TCO materials, including doped and undoped binary, ternary, and quaternary compounds, also suffer from the same limitations. Only some exceptional samples had a resistivity of $\leq1\times10^{-4}$ Ω cm.

In addition to the above mentioned effects that limit the conductivity, high dopant concentration could lead to clustering of the dopant ions, which increases significantly the scattering rate, and it could also produce nonparabolicity of the conduction band, which has to be taken into account for degenerately doped semiconductors with filled conduction bands.

6. Optical properties of TCO

The transmission window of TCOs is defined by two imposed boundaries. One is in the near-UV region determined by the effective band gap Eg, which is blue shifted due to the Burstein–Moss effect. Owing to high electron concentrations involved the absorption edge is shifted to higher photon energies. The sharp absorption edge near the band edge typically corresponds to the direct transition of electrons from the valence band to the conduction band. The other is at the near infrared (NIR) region due to the increase in reflectance caused by the plasma resonance of electron gas in the conduction band. The absorption coefficient (α) is very small within the defined window and consequently transparency is very high. The positions of the two boundaries defining the transmission window are closely related to the carrier concentration. For TCOs, both boundaries defining the transmission window shift to shorter wavelength with the increase of carrier concentration. The blue-shift of the near-UV and near-IR boundaries of the transmission window of GZO as the carrier concentration increased from 2.3×10^{20} cm^{-3} to 10×10^{20} cm^{-3}. The blue-shift of the onset of absorption in the near-UV region is associated with the increase in the carrier concentration blocking the lowest states (filled states) in the conduction band from absorbing the photons. The Burstein–Moss effect owing to high electron concentrations has been widely observed in transmittance spectra of GZO and AZO. A comparable or even larger blue-shift in the transmittance spectra of GZO has been reported with absorption edge at about 300 nm wavelength corresponding to a bang gap of about 4.0 eV. The plasma frequency at which the free carriers are absorbed has a negative correlation with the free carrier concentration.

Consequently, the boundary in the near-IR region also shifts to the shorter wavelength with increase of the free carrier concentration. The shift in the near-IR region is more pronounced than that in the near-UV region. Therefore, the transmission window becomes narrower as the carrier concentration increases. This means that both the conductivity and the transmittance window are interconnected since the conductivity is also related to the carrier concentration as discussed above. Thus, a compromise between material conductivity and transmittance window must be struck, the specifics of which being application dependent. While for LED applications the transparency is needed only in a narrow range around the emission wavelengths, solar cells require high transparency in the whole solar spectral range. Therefore, for photovoltaics, the carrier concentration should be as low as possible for reducing the unwanted free carrier absorption in the IR spectral range, while the carrier mobility should be as high as possible to retain a sufficiently high conductivity. Optical measurements are also commonly employed to gain insight into the film quality. For example, interference fringes found in transmittance curves indicate the highly reflective nature of surfaces and interfaces in addition to the low scattering and absorption losses in the films. The particulars of interferences are related to both the film thickness and the incident wavelength, which can be used to achieve higher transmittance for TCOs. In the case of a low quality TCO, deep level emissions occurring in photoluminescence (PL) spectra along with relatively low transmittance are attributed to the lattice defects such as oxygen vacancies, zinc vacancies, interstitial metal ions, and interstitial oxygen. High-doping concentration-induced defects in crystal lattices causing the creation of electronic defect states in band gap similarly have an adverse effect on transparency. In GZO, as an example, at very high Ga concentrations (10^{20}–10^{21} cm^{-3}), the impurity band merges with the conduction band causing a tail-like state below the conduction band edge of intrinsic ZnO. These tail states are responsible for the low-energy part of PL emission. Therefore, the defects, mainly the oxygen-related ones, in TCOs have to be substantially reduced, if not fully eliminated, through the optimal growth conditions to attain higher transmittance.

7. Application of TCO in solar cells

Solar cells exploit the photovoltaic effect that is the direct conversion of incident light into electricity. Electron–hole pairs generated by solar photons are separated at a space charge region of the two materials with different conduction polarities. Solar cells represent a very promising renewable energy technology because they provide clean energy source (beyond manufacturing) which will reduce our dependence on fossil oil. The principles of operation of solar cells have been widely discussed in detail in the literature and as such will not be repeated here. Rather, the various solar cell technologies will be discussed in the context of conduction oxides. Solar cells can be categorized into bulk devices (mainly single-crystal or large-grain polycrystalline Si), thin film single- and multiple-junction devices, and newly emerged technology which include dye-sensitized cells, organic/polymer cells, high-efficiency multi-junction cells based on III–V semiconductors among others. Crystalline silicon modules based on bulk wafers have been dubbed as the “first-generation” photovoltaic technology. The cost of energy generated by PV modules based on bulk-Si wafers is currently around $3–$4/Wp and cost reduction potential seems limited by the price of Si wafers. This cost of energy is still too high for a significant influence on energy production markets. Much of the industry is focused on the most cost efficient technologies in terms of cost per generated power. The two main strategies to bring down the cost of

photovoltaic electricity are increasing the efficiency of the cells and decreasing their cost per unit area. Thin film devices (also referred to as second generation of solar cells) consume less material than the bulk-Si cells and, as a result, are less expensive. The market share of the thin film solar cells is continuously growing and has reached some 15% in year 2010, while the other 85% is silicon modules based on bulk wafers. Alternative approaches also focused on reducing energy price are devices based on polymers and dyes as the absorber materials, which include a wide variety of novel concepts. These cells are currently less efficient than the semiconductor-based devices, but are attractive due to simplicity and low cost of fabrication.

TCO are utilized as transparent electrodes in many types of thin film solar cells, such as a-Si thin film solar cells, CdTe thin film solar cells, and CIGS thin film solar cells. It should be mentioned that, for photovoltaic applications, a trade-off between the sheet resistance of a TCO layer and its optical transparency should be made. As mentioned above, to reduce unwanted free carrier absorption in the IR range, the carrier concentration in TCO should be as low as possible, while the carrier mobility should be as high as possible to obtain sufficiently high conductivity. Therefore, achieving TCO films with high carrier mobility is crucial for solar cell applications.

7.1 Si thin film solar cells

In addition to the well-established Si technology and non-toxic nature and abundance of Si, the advantage of thin film silicon solar cells is that they require lower amount of Si as compared to the devices based on bulk wafers and therefore are less expensive. Several different photovoltaic technologies based on Si thin films have been proposed and implemented: hydrogenated amorphous Si (a-Si:H) with quasi-direct band gap of 1.8 eV, hydrogenated microcrystalline Si (μc-Si:H) with indirect band gap of 1.1 eV, their combination (micromorph Si), and polycrystalline Si on glass (PSG) solar cells. The first three technologies rely on TCOs as front/back electrodes. This thin film p–i–n solar cell is fabricated in a so-called superstrate configuration, in which the light enters the active region through a glass substrate. In this case, the fabrication commences from the front of the cell and proceeds to its back.

First, a TCO front contact layer is deposited on a transparent glass substrate, followed by deposition of amorphous/microcrystalline Si, and a TCO/metal back contact layer. Therefore, the TCO front contact must be sufficiently robust to survive all subsequent deposition steps and post-deposition treatments. To obtain high efficiency increasing the path length of incoming light is crucial, which is achieved by light scattering at the interface between Si and TCO layers with different refractive indices, so that light is "trapped" within the Si absorber layer. The light trapping allows reduction of the thickness of the Si absorber layer which paves the way for increased device stability. Therefore, TCO layers used as transparent electrodes in the Si solar cells have a crucial impact on device performance. In addition to high transparency and high electrical conductivity, a TCO layer used as front electrode should ensure efficient scattering of the incoming light into the absorber layer and be chemically stable in hydrogen-containing plasma used for Si deposition, and act as a good nucleation layer for the growth of microcrystalline Si. The bottom TCO layer between Si and a metal contact works as an efficient back reflector as well as a diffusion barrier.

To increase light scattering, surface texturing of the front and back TCO contact layers is commonly used. As discussed above, the TCOs for practical applications are ITO, FTO and

GZO/AZO. For reasons mentioned in the text dealing with the discussion of various TCO materials, FTO films have been widely used in solar cells to replace ITO. Alternatively, FTO coated ITO/glass substrate have been proposed to overcome the shortcomings of pure ITO. FTO is the one typically used but cost-effective SnO_2-coated glass substrates on large areas (~1 m^2) are still not being used as a standard substrate. On the other hand, AZO has emerged as a promising TCO material for solar cells. The AZO/glass combination has better transparency and higher conductivity than those of commercial FTO/glass substrates. Another benefit is that AZO is more resistant to hydrogen-rich plasmas used for chemical vapor deposition of thin film silicon layers as compared to FTO and ITO. The AZO films on glass for thin film silicon solar cells have a sheet resistance of about 3Ω/sq for a film thickness of ~1000 nm, a figure which degrades for thinner films. They also reported a transmittance of ~90% in the visible region of the optical spectrum for a film thickness of ~700 nm, which enhances for thinner films. These thin film silicon solar cells all have high external quantum efficiencies in the blue and green wavelength regions due to the good transmittance of the AZO films and good index matching as well as a rough interface for avoiding reflections. The highest external quantum efficiency is about 85% at a wavelength of 500 nm. However, as mentioned earlier, AZO degrades much faster than ITO and FTO in dampheat environment.

7.2 CdTe thin film solar cells

CdTe has a direct optical band gap of about 1.5 eV and high absorption coefficient of $>10^5$ cm^{-1} in the visible region of the optical spectrum, which ensures the absorption of over 99% of the incident photons with energies greater than the band gap by a CdTe layer of few micrometers in thickness. CdTe solar cells are usually fabricated in the superstrate configuration, i.e., starting at the front of the cell and proceeding to the back, as described above for the Si solar cells. CdTe is of naturally p-type conductivity due to Cd vacancies. Separation of the photo-generated carriers is performed via a CdTe/CdS p-n heterojunction. CdS is an n-type material because of native defects, and has a band gap Eg~2.4 eV, which causes light absorption in the blue wavelength range which is undesirable. For this reason, the CdS layer is made very thin and is commonly referred to as a "window layer", emphasizing that photons should pass through it to be absorbed in the CdTe "absorber layer". The basic traditional module of CdTe solar cell is composed of a stack of 'Metal/CdTe/CdS/TCO/glass'. The fabrication begins with the deposition of a TCO layer onto the planar soda lime glass sheet followed by the deposition of the CdS window layer and the CdTe light absorber layer, ~ 5 μm in thickness. Efficiencies of up to 16.5% have been achieved with small-area laboratory cells, while the best commercial modules are presently 10%–11% efficient. The thin CdS window layer poses a problem shared by both CdTe and CIS-based thin film modules, which will be discussed in the next section. Since this layer should be very thin (50–80 nm in thickness), pinholes in CdS provide a direct contact between TCO and the CdS absorber layer, creating short circuits and reducing dramatically the efficiency. This problem is especially severe for CdTe cells, because sulfur readily diffuses into the CdTe layer during post-growth annealing further decreasing the CdS layer thickness.

To mitigate this issue, thin buffer layers made of highly resistive transparent oxides are incorporated between the TCO contact and the CdS window. SnO_2 layers are commonly used as such buffers, although $ZnSnO_x$ films also have been proposed. The exact role of the

buffer layers is not fully understood, whether it simply prevents short circuits by introducing resistance or also changes the interfacial energetics by introducing additional barriers, and optimization of this interface is a critical need. TCO materials typically used in CdTe solar cells are ITO and FTO. Reports for AZO in CdTe cells are very few. The use of ZnO-based TCOs in CdTe solar sells of superstrate configuration is hampered by its thermal instability and chemical reaction with CdS at high temperatures (550–650°C) typically used for CdTe solar cells fabrication. To resolve this problem, Gupta and Compaan applied low temperature (250°C) deposition by magnetron sputtering to fabricate superstrate configuration CdS/CdTe solar sells with AZO front contacts. These cells yielded efficiency as high as 14.0%. Bifacial CdTe solar cells make it possible to increase the device NIR transmission as the parasitic absorption and reflection losses are minimized. The highest efficiency of 14% was achieved from a CdTe cell with an FTO contact layer. The device performance depends strongly on the interaction between the TCO and CdS films. Later, the same group has noted a substantial In diffusion from ITO to the CdS/CdTe photodiode, which can be prevented by the use of undoped SnO_2 or ZnO buffers. Application of TCO as the back contact also allows fabrication of bifacial CdTe cells or tandem cells, which opens a variety of new applications of CdTe solar cells.

7.3 CIGS thin film solar cells

Copper indium diselenide ($CuInSe_2$ or CIS) is a direct-bandgap semiconductor with a chalcopyrite structure and belongs to a group of miscible ternary I–III–VI_2 compounds with direct optical bandgaps ranging from 1 to 3.5 eV. The miscibility of ternary compounds, that is the ability to mix in all proportions, enables quaternary alloys to be deposited with any bandgap in this range. A large light absorption coefficient of $>10^5$ cm^{-1} at photon energies greater than a bandgap allows a relatively thin (few μm in thickness) layer to be used as the light absorber. The alloy systems with optical bandgaps appropriate for solar cells include $Cu(InGa)Se_2$, $CuIn(SeS)_2$, $Cu(InAl)Se_2$, and $Cu(InGa)S_2$. Copper indium–gallium diselenide $Cu(InGa)Se_2$ (or CIGS) has been found to be the most successful absorber layer among chalcopyrite compounds investigated to date. The bandgap is ~1.0 eV for $CuInSe_2$ and increases towards the optimum value for photovoltaic solar energy conversion when gallium is added to produce $Cu(In, Ga)Se_2$. An energy bandgap of 1.25–1.3 eV corresponds to the maximum gap achievable without loss of efficiency. Further increase in the Ga fraction reduces the formation energies of point defects, primary, copper vacancies which makes them more likely to form. Also, a further increase in gallium content makes the absorber layers too highly resistive to be used in solar cells. Therefore, most CIGS devices are produced with an energy bandgap below 1.3 eV, which limits their V_{OC} at ~700 meV. Note that both CIS- and CIGS-based devices are usually dubbed as the CIS technology in the literature. The CIS technology provides the highest performance in the laboratory among all thin-film solar cells, with confirmed power conversion efficiencies of up to 20.1% for small (0.5 cm^2) cells fabricated by the Zentrum fuer Sonnenenrgie-und-Wasserstoff–Forschung and measured at the Fraunhofer Institute for Solar Energy Systems, and many companies around the world are developing a variety of manufacturing approaches aimed at low-cost, high-yield, large-area devices which would maintain laboratory-level efficiencies.

Similarly, TCO layers are generally used for the front contact, whereas a reflective contact material (Ag, frequently in combination with a TCO interlayer, is the most popular one) is needed on the back surface to enhance the light trapping in absorber layers. The optical

quality of these materials substantially affects the required thickness of the absorber layers in terms of providing the absorption of an optimal amount of irradiation. Depending on the application, devices are fabricated in either a ''substrate'' or a ''superstrate'' configuration. The superstrate configuration is based on TCO-coated transparent glass substrates, and the layers are deposited in a reversed sequence, from the top (front) to the bottom (back). The deposition starts with a contact window layer of a photodiode and ends with a back reflector. Light enters the cell through the glass substrate.

In the superstrate configuration, it is important for the TCO as substrate material to be not only electrically conductive and optically transparent, but also be chemically stable during solar-cell material deposition. The superstrate design is particularly suited for building integrated solar cells in which a glass substrate can be used as an architectural element. In the case of the substrate configuration, solar cells are fabricated from the back to the front, and the deposition starts from the back reflector and is finished with a TCO layer. For some specific applications, the use of lightweight, unbreakable substrates, such as stainless steel, polyimide or PET (polyethylene terephtalate) is advantageous.

8. A novel violet and blue enhanced SINP silicon photovoltaic device

8.1 Introduction

Violet and blue enhanced semiconductor photovoltaic devices are required for various applications such as optoelectronic devices for communication, solar cell, aerospace, spectroscopic, and radiometric measurements. Silicon photodetector are sensitive from infrared to visible light but have poor responsivity in the short wavelength region. Since the absorption coefficient of crystal Si is very high for shorter wavelengths in the violet region and is small for longer wavelengths. The heavily doped emitter may contain a dead layer near the surface resulting in poor quantum efficiency of the photoelectric device under short wavelength region.

In order to improve the responsivity of silicon photodiode at the 400-600nm, a novel ITO/SiO_2/np Si SINP violet and blue enhanced photovoltaic device (SINP is the abbreviation of semiconductor/insulator/np structure) was successfully fabricated using thermal diffusion of phosphorus for shallow junction, a very thin silicon dioxide and ITO film as an antireflection/passivation layer. The schematic and bandgap structure of the novel SINP photovoltaic device are whown here (Fig.1 and Fig.2). The very thin SiO_2 film

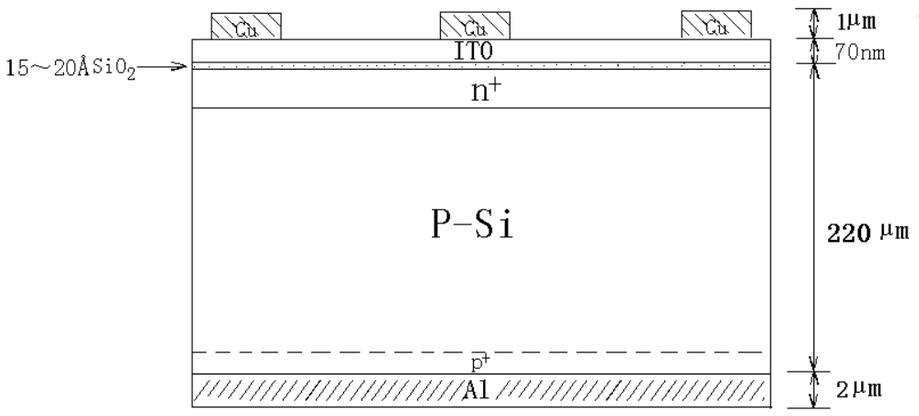

Fig. 1. Schematic of the novel SINP photovoltaic device.

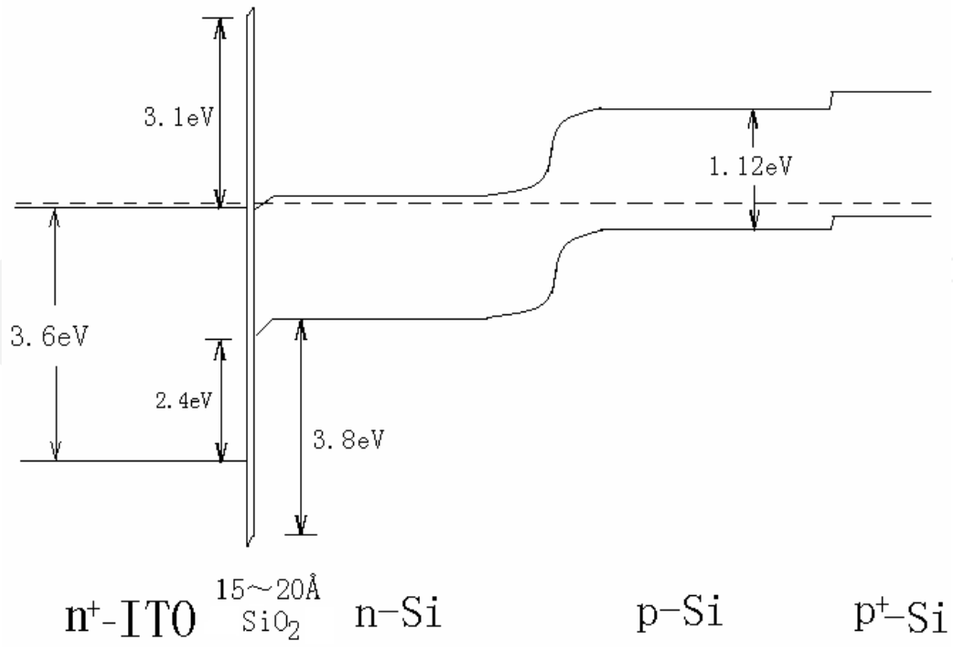

Fig. 2. Bandgap structure of the novel SINP photovoltaic device.

not only effectively passivated the surface of Si, but also reduced the mismatch of ITO and Si. Since a low surface recombination is imperative for good quantum efficiency of the device at short wavelength. The ITO film is high conducting, good antireflective (especially for violet and blue light) and stable. In addition, a wide gap semiconductor as the top film can serve as a low-resistance window, as well as the collector layer of the junction. Therefore, it can eliminate the disadvantage of high sheet resistance, which results from shallow junction. Because the penetration depth of short wavelength light is thin, the shallow junction is in favor of improving sensitivity.

8.2 Experimental in detail

The starting material was 2.0 Ωcm p-type CZ silicon. In the present, two types of shallow and deep junction n-emitters for violet and near-infrared SINP photovoltaic devices were made in an open quartz tube using liquid $POCl_3$ as the doping source. The sheet resistance is 37Ω/□ and 10Ω/□, while the junction depth is 0.35μm and 1μm, respectively. After phosphorus-silicon glass removing, a 2 μm Al metal electrode was deposited on the p-silicon as the bottom electrode by vacuum evaporation. The 15~20Å thin silicon oxide film was successfully grown by low temperature thermally (500°C for 20 min in N_2:O_2=4:1 condition) grown oxidation technology. The 70 nm ITO antireflection film was deposited on the substrate in a RF magnetron sputtering system. Sputtering was carried out at a working gas (pure Ar) pressure of 1.0Pa.

The Ar flow ratio was 30 sccm. The RF power and the substrate temperature were 100W and 300°C, respectively. The sputtering was processed for 0.5h.The ITO films were also prepared on glass to investigate the optical and electrical properties. Finally, by sputtering, a 1μm Cu metal film was deposited with a shadow mask on the ITO surface for the top grids electrode. The area of the device is 4.0 cm^2.

8.3 Results and discussion

8.3.1 Optical and electric properties of ITO films

In order to learn the optical absorption and energy band structure of ITO film, the transmission spectrum of the ITO film deposited on the glass substrate was measured (Fig.3). The thickness of ITO film is about 700 Å. The average transmittance of the film is about 95% in the visible region and the band-edge at 325nm.While the optical band gap of ITO film is about 3.8 eV by calculation. The reflection loss for ITO film on a texturized Si surface was indicated (Fig.4) from UV to the visible regime, which is much lower than that of Si_3N_4 film that are widely made by PECVD technology. This shows that ITO film effectively reduced reflection loss in short-wavelength, which is suitable for antireflection

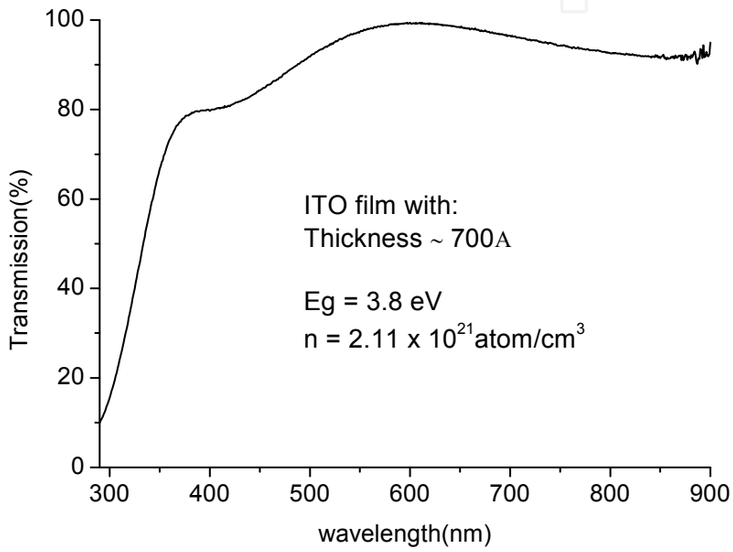

Fig. 3. Transmission spectrum of the ITO film.

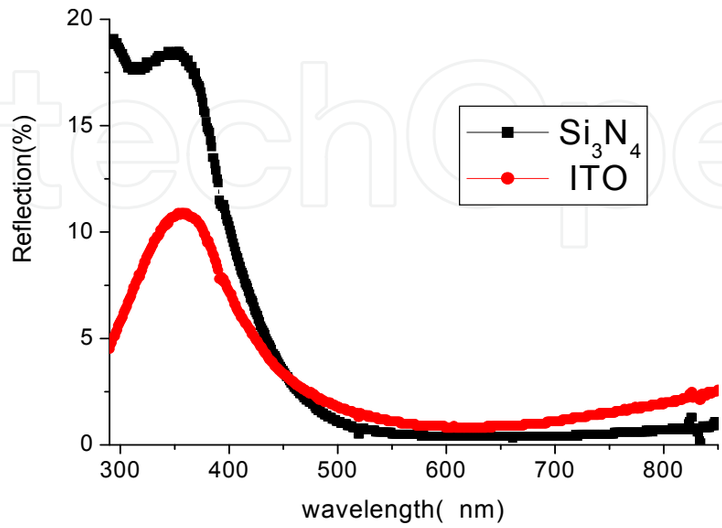

Fig. 4. Comparison of the reflections for ITO and Si_3N_4 films on a texturized Si surface.

coating in violet and blue photovoltaic device. Electrical properties of the ITO film were measured by four-point probe and Hall effect measurement. The square resistance and the resistivity are low to 17Ω/□ and 1.19×10^{-4} Ω·cm, respectively, while carrier concentration is high to 2.11×10^{21} atom/cm^3.

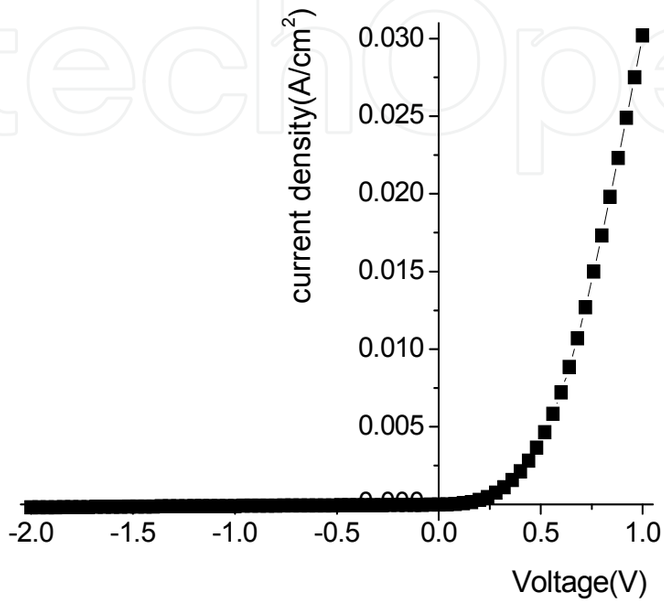

Fig. 5. I-V curve of the violet and blue enhanced (shallow junction) SINP photovoltaic device in dark.

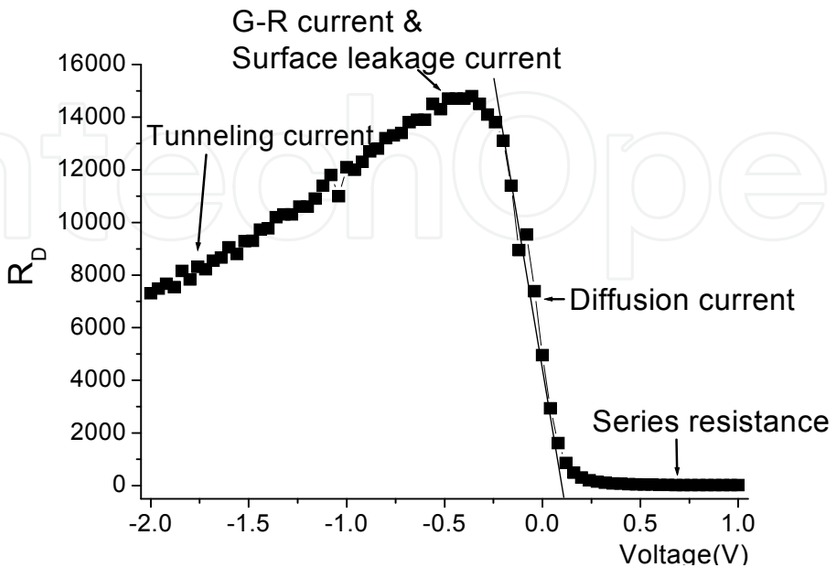

Fig. 6. The variation of resistance for SINP violet device via voltage (R_D-V curve).

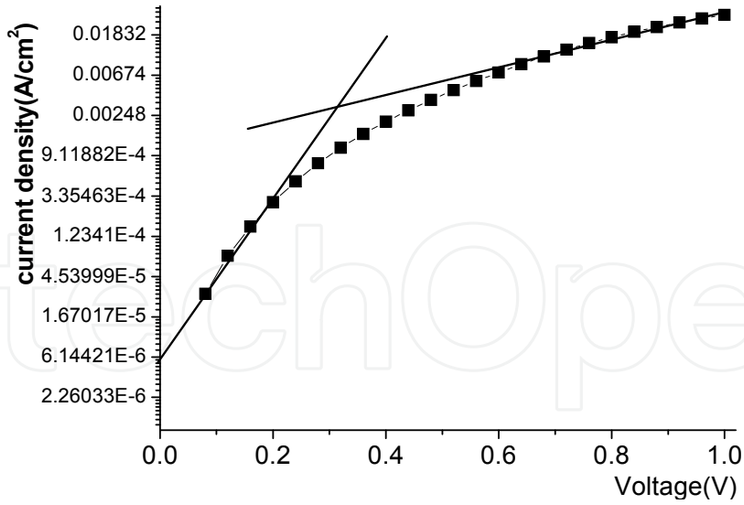

Fig. 7. The corresponding logarithmic scale in current with forward bias condition.

8.3.2 I-V characteristics

In our study, the current-voltage characteristic of the violet SINP device was measured in dark at room temperature (in Fig.5). I-V curves of the devices show fairly good rectifying behaviors. Basing on the dark current as a function of the applied bias, the corresponding diode resistance defined as $R_D = (\frac{dI}{dV})^{-1}$ is derived and shown (in Fig.6). The series resistance arose from ohmic depletion plays a dominant role when the forward bias is larger than 0.25 V. When the voltage varies within 0.2 V and - 0.2 V, the resistance slightly increases as the diffusion current in the base region. When the inversion voltage increases from - 0.2 to - 0.5 V, the leakage current and the recombination current in the surface layers restrain the increase of the dynamic resistance, which keeps the R_D – V curve in an invariation state. In the high inversion voltage region, the tunneling current plays a dominant role.

The plot of ln(J) against V, is shown (in Fig.7), which indicates that the current at low voltage (V < 0.3 V) varies exponentially with voltage. The characteristics can be described by the standard diode equation: $J = J_0(e^{\frac{qV}{nk_BT}} - 1)$ where q is the electronic charge, V is the applied voltage, k_B is the Boltzmann constant, n is the ideality factor and J_0 is the saturation current density. Calculation of J_0 and n from is obtained the measurements (in Fig.7). The value of the ideality factor of the violet SINP device is determined from the slop of the straight line region of the forward bias log(I)-V characteristics. At low forward bias (V< 0.2 V), the typical values of the ideality factors and the reverse saturation current density are 1.84 and 5.58×10^{-6}A/cm², respectively.

Using the standard diode equation $J = J_0(e^{\frac{qV}{nk_BT}} - 1)$, where n = 1.84 and $J_0 = 5.58\times10^{-6}$ A/cm². The result of calculation is similar to that of the measurement (in I-V curve). By the same calculation method, the ideality factor and the reverse saturation current density of deep junction SINP photovoltaic device are 2.21 and 4.2×10^{-6} A/cm², respectively. This result indicates that the recombination current $J_r \approx \exp(qV/2kT)$ dominates in the forward current. The rectifying behaviors and the composition of dark current for violet SINP photovoltaic device is better than deep junction SINP device, because the ideality factor of the violet SINP

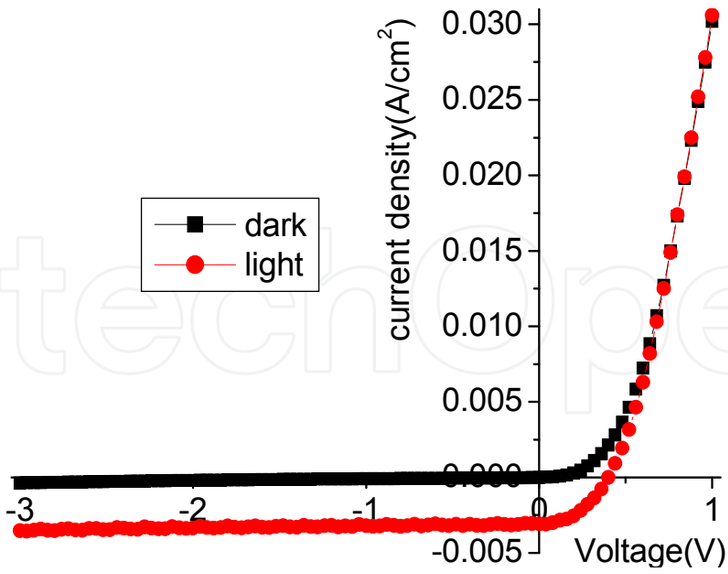

Fig. 8. I-V characteristic of the violet and blue enhanced SINP photovoltaic devices in dark and light (6.3 mW/cm² - white light), respectively.

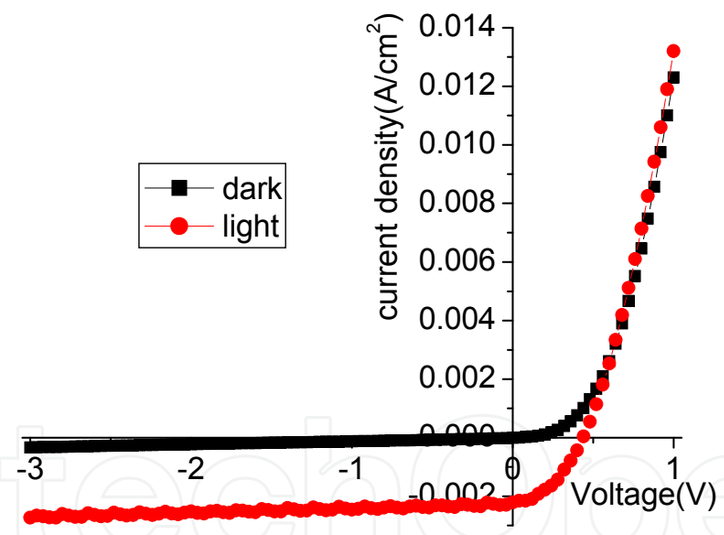

Fig. 9. I-V characteristic of the deep junction SINP devices in dark and light (6.3 mW/cm² - white light), respectively.

photovoltaic device (n=1.84) is lower than that of the deep junction SINP device (n=2.21). Furthermore, the values of I_F/I_R (I_F and I_R stand for forward and reverse current, respectively) at 1V for violet SINP device and deep junction SINP device are found to be as high as 324.7 and 98.4, respectively.

The weak light-injection I-V characteristics of the novel SINP devices with low power white light (6.3mW/cm²) illuminating were measured at 23°C. It is observed that the novel SINP device exhibits a good photovoltaic effect and rectifying behavior in the photon – induced carrieres transportation. On the other side, another essential physical parameter is internal

quantum efficiency (IQE) or external quantum efficiency (EQE) for the evaluation of the spectra response of the light (Fig.8 and Fig.9). The photocurrent density (~ 3.08×10^{-3} A/cm^2) of violet and blue enhanced SINP photovoltaic device is much higher than that of deep junction SINP device (~ $2.23 \times 10^{-3} A/cm^2$), at V = 0.

8.3.3 Spectral response and responsivity

The comparison of IQE, EQE and the responsivity for the violet and blue SINP photovoltaic device and the deep junction SINP photovoltaic device has been illustrated (in Fig.10 ~ Fig.12). In visible light region, the internal and external quantum efficiencies (IQE and EQE) of the devices are in the range of 75% to 85%. In the violet and blue region, the IQE and EQE of shallow junction violet SINP device is much higher than that of the deep junction SINP device. For example, the EQE and the responsivity of the violet SINP device are 70% and 285mA/W at 500nm, respectively, while the EQE and the responsivity of the deep junction SINP device are 42% and 167mA/W at 500nm, respectively. The spectral responsivity peak of violet and blue SINP photovoltaic device is 487mA/W at about 800nm. While the spectral responsivity peak of deep junction SINP photovoltaic device is 471mA/W at about 860nm. The high quantum efficiency and the responsivity of violet and blue enhanced photovoltaic cell attribute to the shallow junction and the good conductive, and the violet and blue antireflection of ITO film.

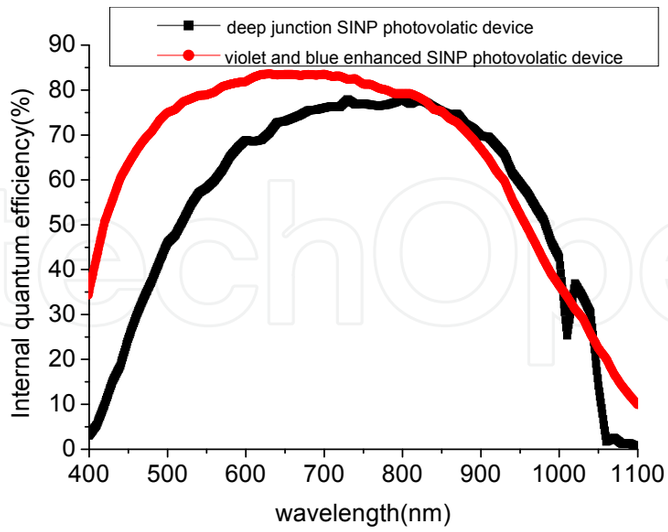

Fig. 10. Comparison of IQE for violet and blue SINP photovoltaic device and the deep junction SINP photovoltaic device.

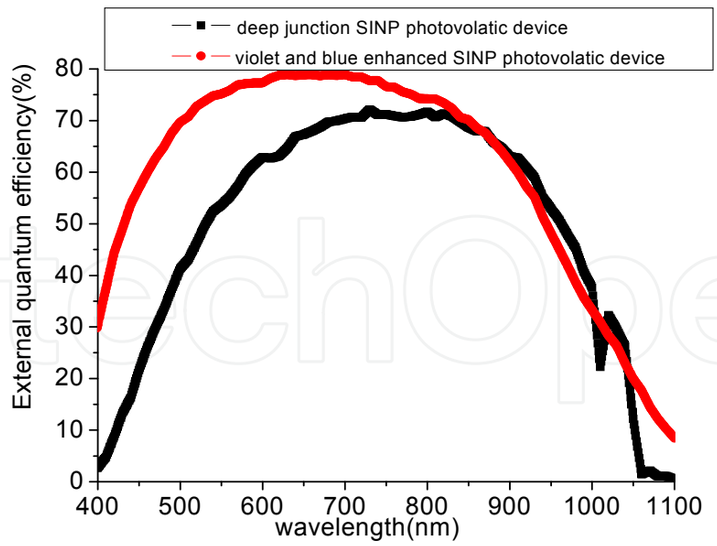

Fig. 11. Comparison of EQE for violet and the blue SINP photovoltaic device and the deep junction SINP photovoltaic device.

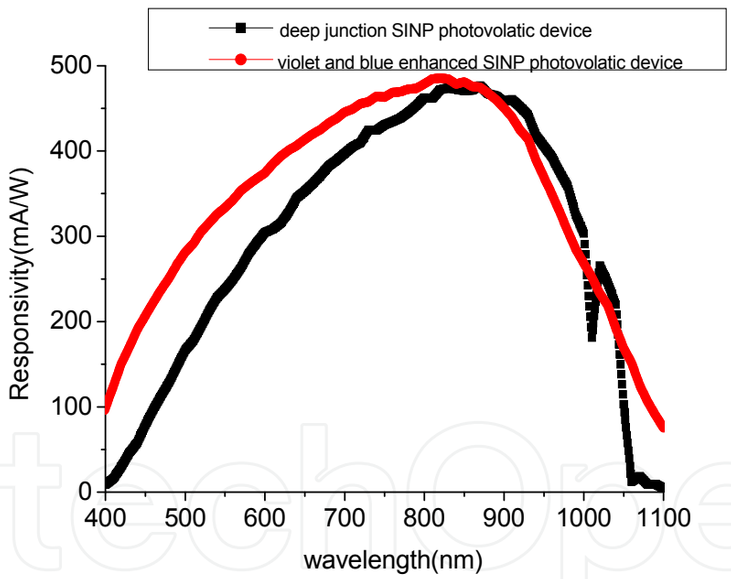

Fig. 12. Comparison of the responsivity for the violet and blue SINP photovoltaic device and the deep junction SINP photovoltaic device.

8.3.4 Conclusions

The novel ITO/SiO_2/np Silicon SINP violet and blue enhanced photovoltaic device has been fabricated by thermal diffusion of phosphorus for shallow junction to enhance the spectral responsivity within the wavelength range of 400-600nm, the low temperature thermally grown a very thin silicon dioxide and RF sputtering ITO antireflection coating to reduce the reflected light and enhance the sensitivity. The ITO film was evinced to a high quality by UV-VIS spectrophotometer, four point probe and Hall-effect measurement. Fairly good

rectifying and obvious photovoltaic behaviors are obtained and analyzed by I-V measurements. The spectral response and the responsivity with a higher quantum efficiency of the violet SINP photovoltaic device and the deep junction SINP photovoltaic device were analyzed in detail. The results indicated that the novel violet and blue enhanced photovoltaic device could be not only used for high quantum efficiency of violet and blue enhanced silicon photodetector for various applications, but also could be used for the high efficiency solar cell.

9. Fabrication and photoelectric properties of AZO/SiO_2/p-Si heterojunction device

9.1 Introduction

As shown in the previous work, semiconductor-insulator-semiconductor (SIS) diodes have certain features, which make them more attractive for the solar energy conversion than conventional Shottky, MIS, or other heterojunction structures (Mridha et al., 2007). For example, efficient SIS solar cells such as indium tin oxide (ITO) on silicon have been reported, where the crystal structures and the lattice parameters of Si (diamond, a = 0.5431 nm), SnO_2 (tetragonal, a = 0.4737 nm, c = 0.3185 nm), In_2O_3 (cubic, a = 1.0118 nm) show that they are not particularly compatible and thus not likely to form good devices. However, the SIS structure is potentially more stable and theoretically more efficient than either a Schottky or a MIS structure. The origins of this potential superiority are the suppression of majority-carrier tunneling in the high potential barrier region of SIS structure, and the existence of thin interface layer which minimizes the amount and the impact of the interface states. This results in an extensive choice of the p-n junction partner with a matching band gap in the front layer. In addition, the top semiconductor film can serve as an antireflection coating (Dengyuan et al., 2002), a low-resistance window, and the collector of the p-n junction as well.

Furthermore, the semiconductor with a wide band gap as the top layer of SIS structure can eliminate the surface dead layer which often occurs within the homojunction devices, such as the normal bulk silicon based solar cells. On the other side, this absence of the light absorption of visible region in a surface layer can improve the ultraviolet response of the internal quantum efficiency. Among many transparent conductive oxides (TCO) of the transition metals, ZnO:Al is one the best n-type semiconductor layer. It has high conductivity, high transmittance, optimized surface texture for light trapping, and large band gap of $E_g \approx 3.3$ eV. Thus, in this description, we show a photovoltaic device with AZO/SiO_2/p-Si frame, as an attempt to study its opto-electronic conversion property and the I-V features as well. The schematic and the bandgap structure of the novel AZO/SiO_2/p-Si SIS heterojunction device was show here (Fig.13).

9.2 Experimental in details

For the purpose of fabricating SIS structure, p-type Si (100) wafers were used as the substrates of the heterojunction device. The wafers were firstly prepared by a stand cleaning procedure, then, they were dipped in 10% HF solution for one minute to remove native oxide layer. Finally, the wafers were dried in a flow gas of nitrogen.

By thermal evaporation, 1 μm-thick Al electrode was deposited on the back side. Then the samples were annealed at 500°C for 20 min in N_2:O_2=4:1 condition to form good ohmic contact and a very thin oxide layer (about 15～20Å) was grown on the p-Si surface.

The Al doped ZnO films were deposited on the oxidized silicon substrates in a RF magnetron sputtering system. The target was a sintered ceramic disk of ZnO doped with 2 wt% Al_2O_3 (purity 99.99%). The base pressure inside the chamber was pumped down to less than 5×10^{-4} Pa. Sputtering was carried out at a working gas (pure Ar) pressure of 1Pa. The Ar flow ratio was 30 sccm. The RF power and the temperature on substrates were kept at 100W and 300°C, respectively. The sputtering was proceeded for 2.5 hours. The area is 2×2 cm^2.

The thickness of AZO film was measured by step profiler. The optical transmission of the films was measured by UV-VIS spectrophotometer. The electrical properties of Al doped ZnO films were characterized by four point probe. The current-voltage characteristics of the device was measured by Agilent 4155C semiconductor parameter analyzer (with probe station, the point diameter of a probe is 5 μm).

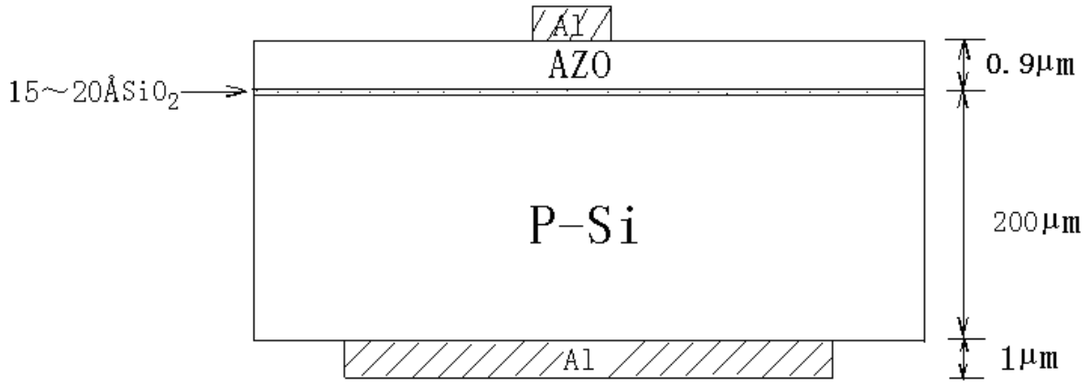

Fig. 13. The structure of AZO/SiO_2/p-Si heterojunction PV device.

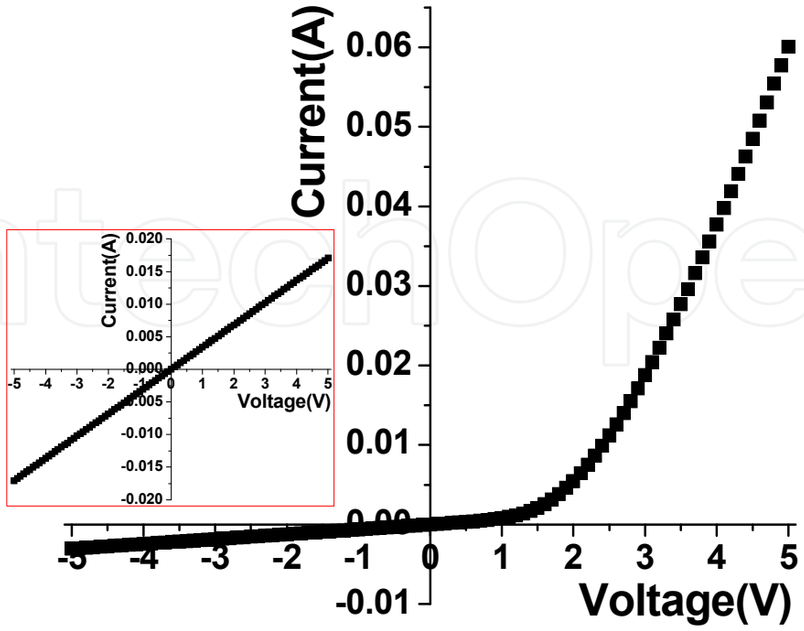

Fig. 14. I-V curve of the Al/AZO/SiO_2/p-Si/Al heterojunction device in dark.

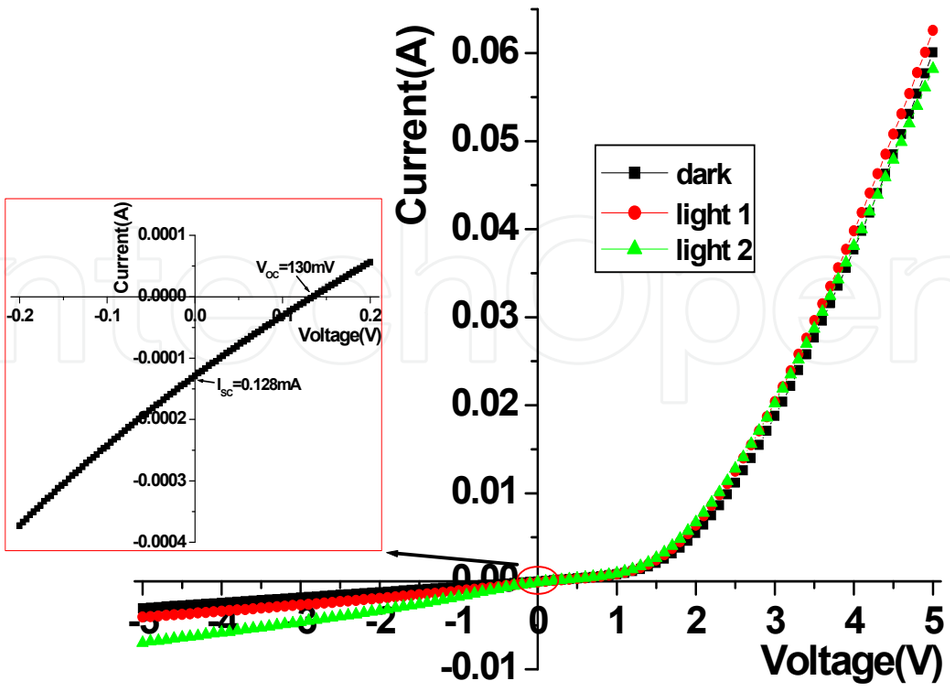

Fig. 15. I-V characteristic of the AZO/SiO_2/p-Si/Al heterojunction device in dark and light (light-1: 6.3mW/cm^2 white light; Light-2: 20W halogen lamp)

9.3 I-V characteristics

A linear I-V behavior between the two electrodes on the surface of ZnO:Al film indicates a good ohmic contact. The current-voltage characteristic of the AZO/SiO_2/p-Si/Al heterojunction device was measured at room temperature in the dark (Fig.14). Typical rectifying is observed for this heterojunction with polar to covalent semiconductors structure. The weak photon irradiation I-V characteristics were measured under two kinds of illumination by low power white light (6.3mW/cm^2) lamp and 20W halogen lamp (in Fig.15). The good rectifying with the increase of photoelectric current was observed for the typical interface mismatching device. Under reverse bias conditions the photocurrent caused by the ZnO surfaces exposing in the low power white light lamp and 20W halogen lamp was obviously much larger than the dark current. For example, when the reverse bias is -5V, the dark current is only 3.05×10^{-3}A.While the photocurrent reach to 4.06×10^{-3}A and 6.99×10^{-3}A under low power white light and halogen lamp illumination, respectively.

9.4 Conclusions

The novel AZO/SiO_2/p-Si/ heterojunction has been fabricated by magnetron sputtering deposition AZO film on p-Si substrate. Fairly good rectifying and photoelectric behaviors are observed and analyzed by I-V measurements in detail. The ideality factor and the saturation current of this diode is 20.1 and 1.19×10^{-4}A, respectively. The results indicated that the novel AZO/SiO_2/p-Si/ heterojunction device could be not only used for low cost solar cell, but also could be used for the high quantum efficiency enhanced photodiode in UV and visible lights, and also for other applications.

10. References

Ashok, S.; Sharma, P.P.; Fonash, S.J. (1980) IEEE Transactions on Electron Devices 27, (1980) pp. 725-730

Bruk, L.; Fedorov, V.; Sherban, D.; Simashkevich, A.; Usatii, I.; Bobeico, E.; Morvillo, P. (2009) "Isotype bifacial silicon solar cells obtained by ITO spray pyrolysis", Materials Science and Engineering B 159–160 (2009) pp.282–285

Baik, D.G.; Cho, S.M. (1999). "Application of sol-gel derived films for ZnO/n-Si junction solar cells, Thin Solid Films 354 (1999) pp.227-231

Chaabouni, F.; Abaab, M. Rezig, B. (2006). "Characterization of n-ZnO/p-Si films grown by magnetron sputtering", Superlattices and Microstructures, vol 39, (2006) pp.171-178

Cheknane, Ali (2009) "Analytical modelling and experimental studies of SIS tunnel solar cells", J. Phys. D: Appl. Phys. 42 (2009) pp.115302-115307

Chen, X. D.; Ling, C. C.; Fung, S.; Beling, C. D. (2006). "Current transport studies of ZnO/p-Si heterostructures grown by plasma immersion ion implantation and deposition", Applied Physics Letters, vol 88, (2006) pp.132104-132107

Canfield, L.R.; Kerner, J.; Korde, R. (1990). "Silicon photodiodes optimized for the EUV and soft xray regions", EUV.X-Ray.andGamma-Ray Instrumentation for Astronomy. SPIE vol 1344 , (1990) pp. 372—377

Granqvist, C.G. (2007) "Transparent conductors as solar energy materials: A panoramic review", Sol. Ener. Mater. Sol. Cells 91, (2007) pp.1529-1598

Granqvist, Claes G. (2007) "Transparent conductors as solar energy materials: A panoramic review", Solar Energy Materials & Solar Cells 91 (2007) pp.1529–1598

He, B.; Ma, Z.Q. et al., (2009). "Realization and Characterization of ITO/AZO/SiO_2/p-Si SIS Heterojunction", Superlattices and Microstructures 46, (2009) pp.664-671

He, B.; Ma, Z.Q. et al., (2010). "Investigation of ultraviolet response enhanced PV cell with silicon-based SINP configuration", SCIENCE CHINA Technological Sciences 53, (2010) pp.1028-1037

Koida, T.; Fujiwara, H.; Kondo, M. (2009) "High-mobility hydrogen-doped In_2O_3 transparent conductive oxide for a-Si:H/c-Si heterojunction solar cells", Solar Energy Materials & Solar Cells 93 (2009) pp.851–854

Kittidachachan, P.; Markvart, T.; Ensell, G.J.; Greef, R.; Bagnall, D.M. (2005). "An analysis of a "dead layer" in the emitter of n+pp+ solar cells", Photovoltaic Specialists Conference, Conference Record of the Thirty-first IEEE, vol 3-7, (Jan., 2005) pp. 1103-1106

Mridha, S.; Basak, Durga. (2007). "Ultraviolet and visible photoresponse properties of n-ZnO/p-Si heterojunction", Journal of Applied Physics, Vol 101, (2007) pp.083102

Ramamoorthy, K.; Kumar, K.; Chandramohan, R.; Sankaranarayanan, K. (2006) "Review on material properties of IZO thin films useful as epi-n-TCOs in opto-electronic (SIS solar cells, polymeric LEDs) devices", Materials Science and Engineering B 126 (2006) pp.1–15

Song, Dengyuan; Aberle, Armin G.; Xia, James (2002). "Optimisation of ZnO:Al films by change of sputter gas pressure for solar cell application", Applied Surface Science 195, (2002) pp.291-296

Singh, R.; Rajkanan, K.; Brodie, D.E.; Morgan, J.H. (1980) IEEE Transactions on Electron Devices 27, (1980) pp. 656-662

Wenas, Wilson W.; Riyadi, S. (2006). "Carrier transport in high-efficiency ZnO/SiO_2/Si solar cells", Solar Energy Materials and Solar Cells 90，(2006) pp.3261-3267

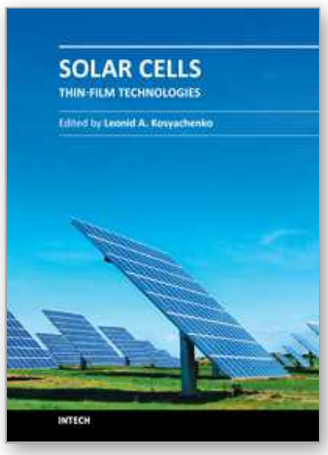

Solar Cells - Thin-Film Technologies

Edited by Prof. Leonid A. Kosyachenko

ISBN 978-953-307-570-9
Hard cover, 456 pages
Publisher InTech
Published online 02, November, 2011
Published in print edition November, 2011

The first book of this four-volume edition is dedicated to one of the most promising areas of photovoltaics, which has already reached a large-scale production of the second-generation thin-film solar modules and has resulted in building the powerful solar plants in several countries around the world. Thin-film technologies using direct-gap semiconductors such as CIGS and CdTe offer the lowest manufacturing costs and are becoming more prevalent in the industry allowing to improve manufacturability of the production at significantly larger scales than for wafer or ribbon Si modules. It is only a matter of time before thin films like CIGS and CdTe will replace wafer-based silicon solar cells as the dominant photovoltaic technology. Photoelectric efficiency of thin-film solar modules is still far from the theoretical limit. The scientific and technological problems of increasing this key parameter of the solar cell are discussed in several chapters of this volume.

InTech Europe
University Campus STeP Ri
Slavka Krautzeka 83/A
51000 Rijeka, Croatia
Phone: +385 (51) 770 447
Fax: +385 (51) 686 166
www.intechopen.com

InTech China
Unit 405, Office Block, Hotel Equatorial Shanghai
No.65, Yan An Road (West), Shanghai, 200040, China
中国上海市延安西路65号上海国际贵都大饭店办公楼405单元
Phone: +86-21-62489820
Fax: +86-21-62489821

IntechOpen